European Journal of Medicinal Chemistry 46 (2011) 2397–2407

Contents lists available at ScienceDirect

European Journal of Medicinal Chemistry

journal homepage: http://www.elsevier.com/locate/ejmech

Original article

Facile synthesis, vasorelaxant properties and molecular modeling studies of 2-amino-8*a*-methoxy-4*H*-pyrano[3,2-*c*]pyridine-3-carbonitriles

Adel S. Girgis [a,*], Nasser S.M. Ismail [b], Hanaa Farag [a]

[a] *Pesticide Chemistry Department, National Research Centre, Dokki, Cairo 12622, Egypt*
[b] *Pharmaceutical Chemistry Department, Faculty of Pharmacy, Ain Shams University, Cairo, Egypt*

ARTICLE INFO

Article history:
Received 16 January 2011
Received in revised form
6 March 2011
Accepted 12 March 2011
Available online 23 March 2011

Keywords:
4-Piperidones
Ylidenemalononitriles
4*H*-Pyrano[3,2-*c*]pyridine-3-carbonitriles
Vasodilation
Molecular modeling

ABSTRACT

A facile synthetic approach towards 6-alkyl-2-amino-4-aryl-4*a*,5,6,7,8,8*a*-hexahydro-8*a*-methoxy-4*H*-pyrano[3,2-*c*]pyridine-3-carbonitriles **3a**–**n** was reported via reaction of 1-alkyl-4-piperidones **1a**,**b** with ylidenemalononitriles **2a**–**h** in methanol in the presence of sufficient amount of sodium. The structure of **3** was established through different spectroscopic techniques and confirmed by single crystal X-ray studies. Vasodilation activities of the synthesized compounds were investigated in vitro using isolated thoracic aortic rings of Wister rats pre-contracted with norepinephrine hydrochloride standard method. All the prepared analogues exhibited considerable vasodilation properties especially, **3g** and **3c** which revealed the best vasodilation potency ($IC_{50} = 0.30$, 0.37 mM, respectively) among all the tested compounds. Molecular modeling studies, including fitting of the synthesized compounds to a 3D-pharmacophore and their docking into optimized homology model as α_1-AR antagonists showed high docking score and fit values. The experimental vasodilation activities of compounds **3a**–**n** are consistent with their molecular modeling results.

1. Introduction

Cardiovascular diseases are the main cause of death in most countries. One of the main reasons in cardiovascular diseases is vascular tissues that may lose their capacity to relaxation. Therefore, vascular studies have been paid much attention and the vasodilator agents would be beneficial in treating cardiovascular diseases [1–5]. Relaxation of vascular smooth muscle is the basis for the treatment of hypertension [6]. Hypertension is the most common cardiovascular disease and the one which represents the major risk factor for coronary artery disease, heart failure, stroke and renal failure [7]. The reduction in blood pressure achieved with most of the currently used antihypertensive agents, such as angiotensin-converting enzyme inhibitors, calcium antagonists, β-blockers and diuretics, is directly or indirectly related to the relaxation of the vascular smooth muscle [6,8]. Few publications reported the antihypertension, smooth muscle relaxation and vasodilation properties of pyrano[3,2-*c*]pyridines [9–11]. In the present work, it is intended to report our investigations towards novel synthesis of 4*H*-pyrano[3,2-*c*]pyridine-3-carbonitrile analogues utilizing a facile synthetic pathway and easily accessible starting agents. Vasodilation properties of the prepared analogues will be also discussed. The present study is considered a continuation to our earlier work directed towards construction of novel bio-active agents [12–22] especially, as vasodilators [23–25]. The reported pharmacological properties of pyrano[3,2-*c*]pyridine derivatives as anti-tumor [26,27], antioxidant [28], antiviral [27] as well as antimycobacterial [29] also prompted the present study. Molecular modeling studies including, fitting to a generated 3D-pharmacophore and docking into optimized homology model as α_1-adrenoceptor (α_1-AR) antagonists will be also considered in the present work to explore the intermolecular interactions between the test set and the target protein that validate the observed pharmacological properties and distinguish the attained structure–activity relationships.

2. Results and discussion

2.1. Chemistry

Reaction of 1-alkyl-4-piperidones **1a**,**b** with ylidenemalononitriles **2a**–**h** in methanol in the presence of sufficient amount of sodium afforded colorless to yellow products. The structures of which were established to be 6-alkyl-2-amino-4-aryl-4*a*,5,6,7,8,8*a*-hexahydro-8*a*-methoxy-4*H*-pyrano[3,2-*c*]pyridine-3-carbonitriles **3a**–**n** rather than 2-amino-4*H*-pyrano[3,2-*c*]pyridine-3-carbonitriles **4** or 2-methoxy

* Corresponding author. Tel.: +20 120447199; fax: +20 33370931.
E-mail address: girgisas10@yahoo.com (A.S. Girgis).

0223-5234/$ – see front matter © 2011 Elsevier Masson SAS. All rights reserved.
doi:10.1016/j.ejmech.2011.03.023

[1,6]naphthyridine-3-carbonitriles **5** [19,30–34] based on spectroscopic (IR, ^{1}H, ^{13}C NMR, ^{1}H, ^{1}H-COSY and HMQC) and elemental analyses data (Scheme 1).

The IR spectra of **3a**–**n** reveal the absence of any band assignable for carbonyl function. However, amino stretching vibration bands at $\nu = 3420–3122$ cm^{-1} beside, a strong nitrile stretching vibration band at $\nu = 2189–2174$ cm^{-1} are well recognized. ^{1}H NMR spectrum of **3c** "as a representative example" adds a good support for the established structure, exhibiting the protons of the methylene groups H_2C-5, H_2C-7 and H_2C-8 (at $\delta = 1.88–1.99$, 2.34–2.37; 2.11, 2.72–2.78 and 1.79, 2.28, respectively) as non-magnetically equivalent ones coupled with each other and in turn with the vicinal proton(s). Meanwhile, the methine protons *H*-4*a* and *H*-4 are overlapped with the upfield *H*-5 and methoxide proton signals, respectively. ^{1}H, ^{1}H-COSY spectrum of **3c** (Fig. 1) supports these assignments.

^{13}C NMR (on-resonance & APT) spectra of **3c** "as a representative example of the synthesized compounds" confirm the established structure revealing the methylene carbons *C*-5, *C*-7 and *C*-8 at $\delta = 54.8$, 51.3 and 29.7, respectively. However, the methine carbons *C*-4 and *C*-4*a* are located at $\delta = 37.9$ and 45.0, respectively. HMQC spectrum of **3c** (Fig. 2) adds a strong evidence for these interpretations. Also, ^{13}C NMR (on-resonance) spectra of **3d** and **3i** add good support for the assigned structures (*c.f.* Experimental section). Single crystal X-ray studies of **3c**, **3d** and **3i** (Figs. 3–5) add good confirmations for the established structures exhibiting that the piperidinyl and pyranyl systems are distorted chair form configurations. Theoretical calculations were processed by both AM1 and PM3 methods to compare the observed geometric parameters "geometric parameters obtained experimentally through single crystal X-ray studies and theoretically calculated ones with both AM1 and PM3 methods are presented in Table 1 of supplementary material". The geometries were optimized by the molecular mechanics force field (MM+) followed by either semi-empirical AM1 [35] or PM3 [36,37] methods implemented in the HyperChem

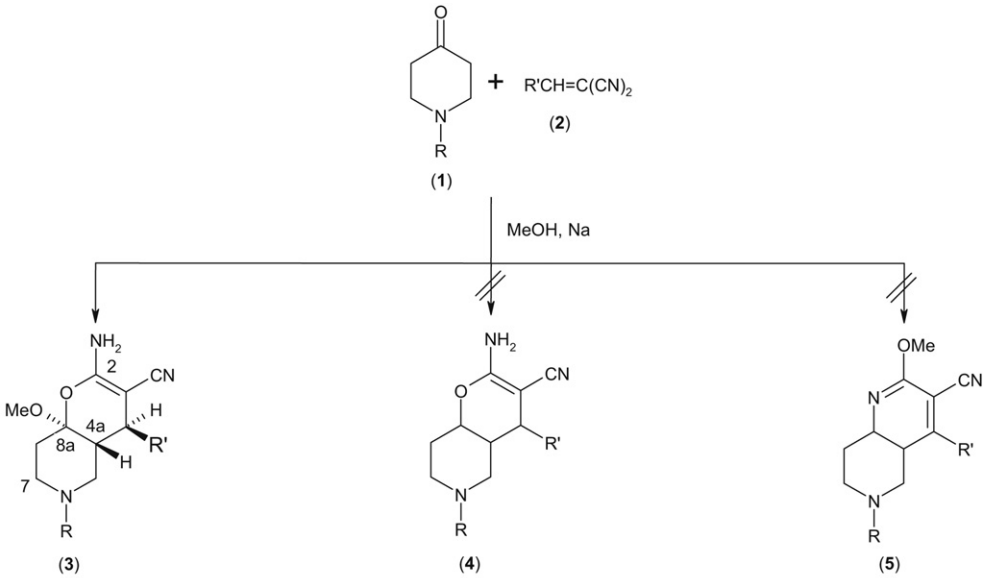

1a; R = Me

1b; R = Et

2a; R' = Ph

2b; R' = 4-ClC_6H_4

2c; R' = 4-FC_6H_4

2d; R' = 4-$H_3CC_6H_4$

2e; R' = 4-$H_3COC_6H_4$

2f; R' = 2-thienyl

2g; R' = 4-(1-piperidinyl)phenyl

2h; R' = 4-(4-morpholinyl)phenyl

3a; R = Me, R' = Ph

3b; R = Et, R' = Ph

3c; R = Me, R' = 4-ClC_6H_4

3d; R = Et, R' = 4-ClC_6H_4

3e; R = Me, R' = 4-FC_6H_4

3f; R = Me, R' = 4-$H_3CC_6H_4$

3g; R = Me, R' = 4-$H_3COC_6H_4$

3h; R = Et, R' = 4-$H_3COC_6H_4$

3i; R = Me, R' = 2-thienyl

3j; R = Et, R' = 2-thienyl

3k; R = Me, R' = 4-(1-piperidinyl)phenyl

3l; R = Et, R' = 4-(1-piperidinyl)phenyl

3m; R = Me, R' = 4-(4-morpholinyl)phenyl

3n; R = Et, R' = 4-(4-morpholinyl)phenyl

Scheme 1.

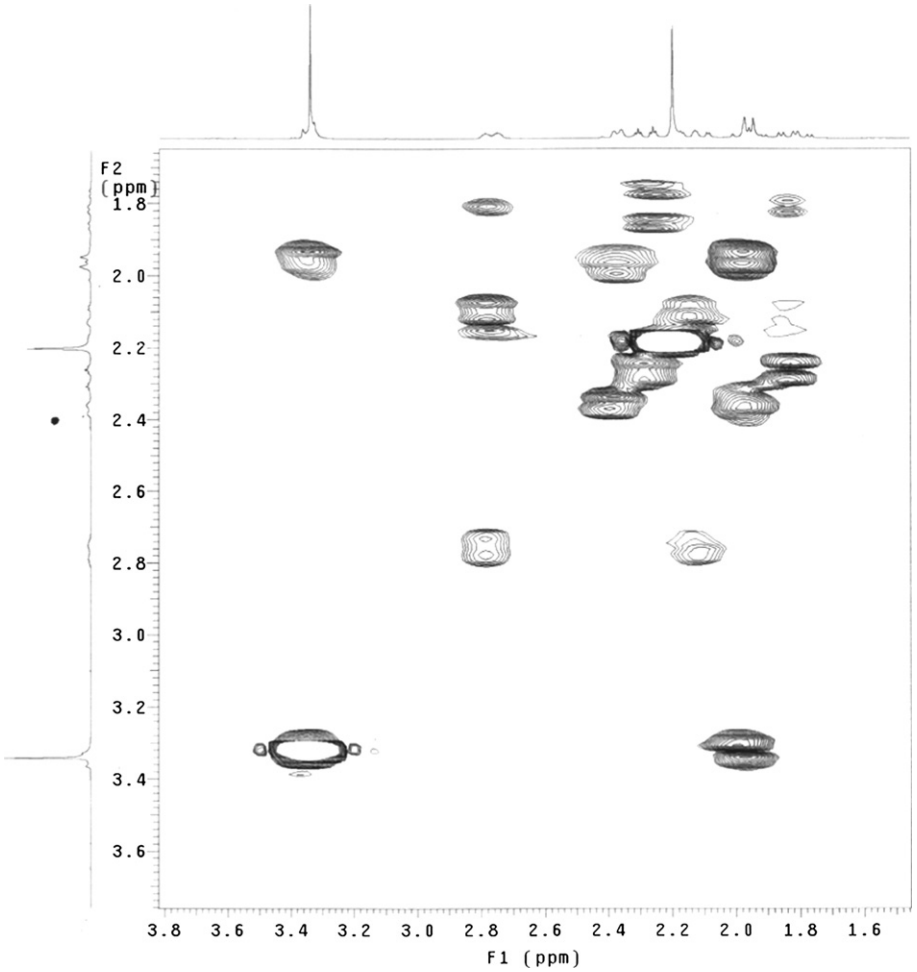

Fig. 1. ^{1}H, ^{1}H-COSY spectrum of **3c**.

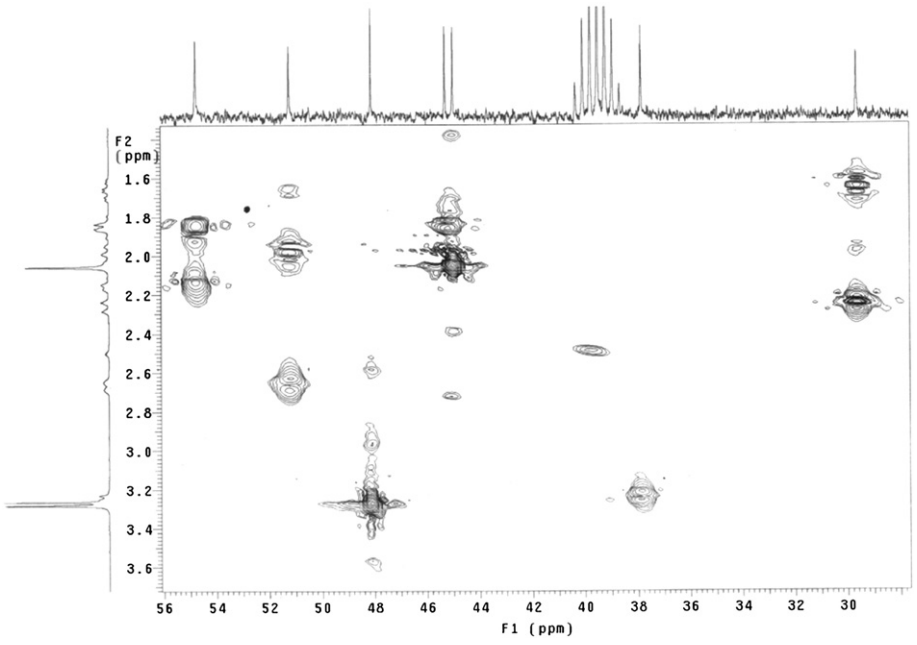

Fig. 2. HMQC spectrum of **3c**.

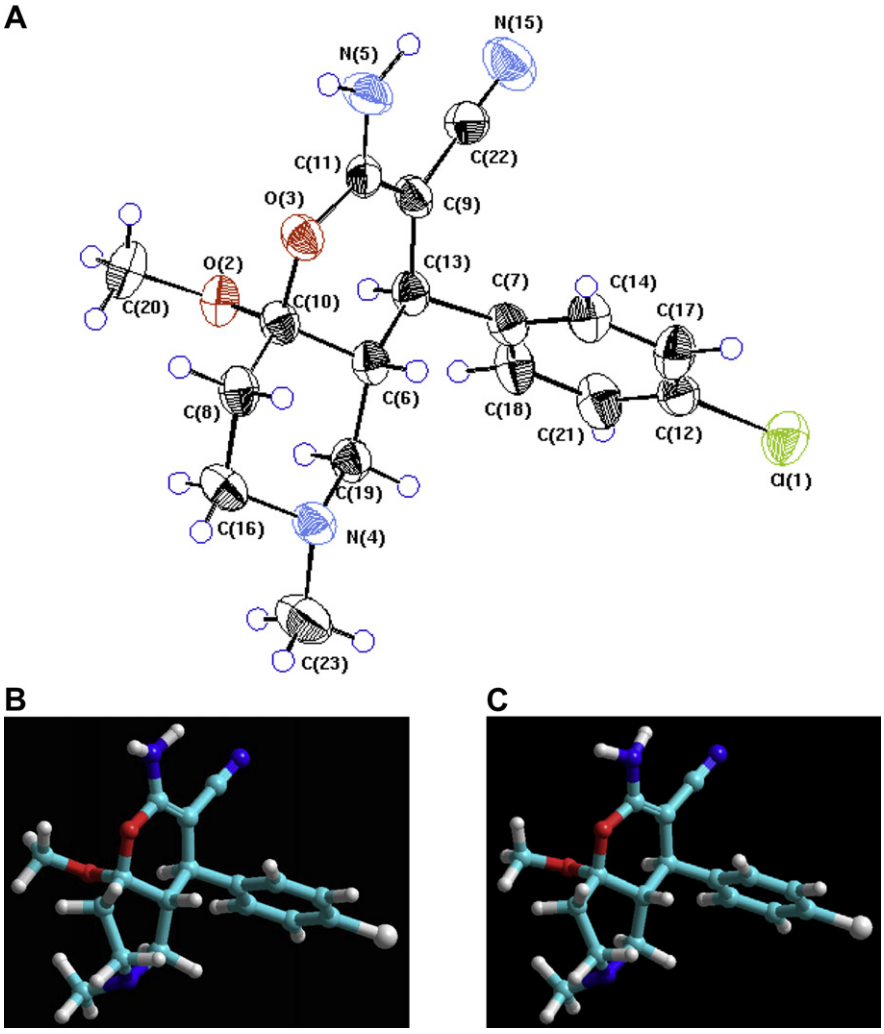

Fig. 3. (A) ORTEP projection of single crystal X-ray diffraction of **3c**; (B), (C) optimized structure of **3c** by semi-empirical AM1 and PM3, respectively.

8.0 package. The structures were fully optimized without fixing any parameters, thus bringing all geometric variables to their equilibrium values. The energy minimization protocol employed the Polak–Ribiere conjugated gradient algorithm. Convergence to a local minimum was achieved when the energy gradient was $\leq$0.01 kcal mol^{-1}. The RHF method was used in the spin pairing for the two semi-empirical tools [38] (Figs. 3–5).

The reaction was assumed to take place via active methylene nucleophilic attack of the 4-piperidone **1** at the β-carbon of unsaturated dinitrile system **2** under the effect of the used basic catalysis, followed by methoxide nucleophilic attack at the carbonyl function with subsequent cyclization due to interaction with the neighboring nitrile group furnishing finally 2-amino-4-aryl-4*a*,5,6,7,8,8*a*-hexahydro-8*a*-methoxy-4*H*-pyrano[3,2-*c*]pyridine-3-carbonitrile **3** (Scheme 2).

2.2. Vasodilation properties

Vasodilation activities of the synthesized pyrano[3,2-*c*]pyridine-3-carbonitrile derivatives (**3a**–**n**) were investigated in vitro using isolated thoracic aortic rings of Wister rats pre-contracted with norepinephrine hydrochloride according to the standard known procedure [23–25,39,40] and compared with prazosin hydrochloride, which was used as a reference standard. From the observed results (Table 1, see also Figs. 1, 2 of the supplementary material), it has been noticed that all the tested analogues show considerable vasodilation properties. Compounds **3g** and **3c** reveal the best vasodilation potency (IC_{50}, concentration necessary for 50% reduction of maximal norepinephrine hydrochloride induced contracture = 0.30, 0.37 mM, respectively) among all the tested analogues. Structure–activity relationship based on the observed results, indicates that the substituent attached at the 4-position of pyrano[3,2-*c*]pyridine-3-carbonitriles plays an important role in developing the observed total vasodilation behavior. Generally (except, in case of **3m**), it has been noticed that substitution of the phenyl group oriented at the 4-position of the constructed heterocycles with either electron-withdrawing (chlorine or fluorine) or electron-donating (methyl, methoxy, piperidinyl or morpholinyl) function, can assist in enhancing the observed pharmacological behavior as exhibited in compounds **3a**,**3c**,**3e**,**3f**,**3g**,**3k** (IC_{50} = 0.72, 0.37, 0.52, 0.60, 0.30 and 0.45 mM, respectively) and **3b**,**3d**,**3l**,**3n** (IC_{50} = 0.68, 0.40, 0.48 and 0.64 mM, respectively). Also, replacement of the phenyl group with a thienyl residue (which is considered its bio-isostere) seems preferable for developing a more pharmacological active agent as exhibited in pairs **3a**,**3i** (IC_{50} = 0.72, 0.68 mM, respectively) and **3b**,**3j** (IC_{50} = 0.68, 0.49 mM, respectively). It has also been noticed that (except in case of **3g**), adoption of chlorine atom as a substituent attached to the phenyl group oriented at the 4-position of the prepared heterocycles, seems the most suitable choice for developing high vasodilation active targets comparable with the other tested residues, as exhibited in

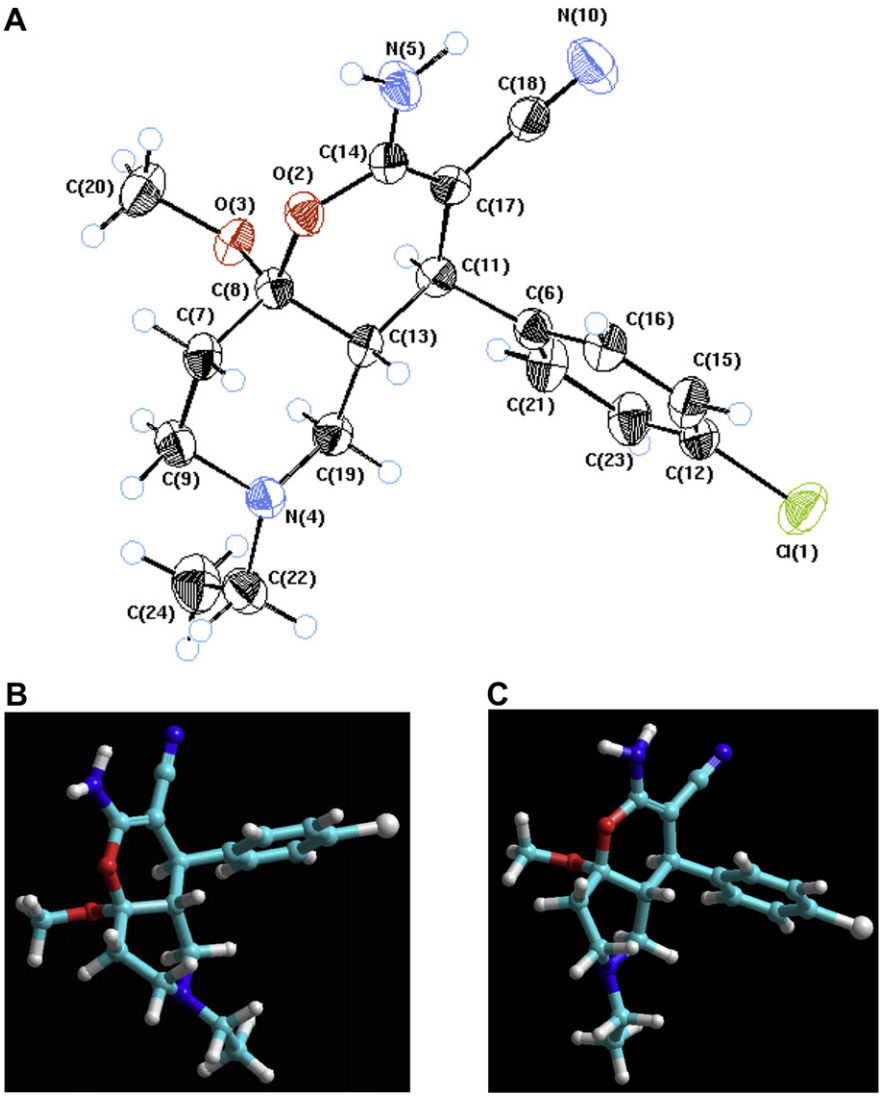

Fig. 4. (A) ORTEP projection of single crystal X-ray diffraction of **3d**; (B), (C) optimized structure of **3d** by semi-empirical AM1 and PM3, respectively.

compounds **3c**,**3e**,**3f**,**3k**,**3m** ($IC_{50} = 0.37$, 0.52, 0.60, 0.45 and 0.74 mM, respectively) and **3d**,**3h**,**3l**,**3n** ($IC_{50} = 0.40$, 0.68, 0.48 and 0.64 mM, respectively). However, no precise rule could be attained through the screened results concerning the role of alkyl chain length (either methyl or ethyl) attached at the 6-position of the constructed heterocycles in affecting the observed pharmacological properties.

2.3. Molecular modeling

Pharmacophore generation as well as docking of antagonists into minimized homology model of receptor were performed using the Discovery Studio 2.5 software (Accelrys Inc., San Diego, CA, USA).

2.3.1. Studies of the pharmacophore/receptor mode of α_1-AR antagonist

The simulation compare/fit study of compounds **3a**–**n** was carried out using our recently reported common feature pharmacophore model that encompassed five features namely; positive ionizable (PI), hydrogen bond acceptor (HBA) and three hydrophobic features (HY1, HY2 and HY3) (see Fig. 3 of the supplementary material) [23]. The structures of the test set of 6-alkyl-2-amino-4-aryl-4*a*,5,6,7,8,8*a*-hexahydro-8*a*-methoxy-4*H*-pyrano[3,2-*c*]pyridine-3-carbonitriles (**3a**–**n**) were built, energy minimized using prepare ligand protocol and their conformational models were generated in the energy range of 20 kcal/mol above the estimated global energy minima. The fitting of the tested compound was performed using best fit during the compare/fit process. Different mappings for all the conformers of each compound of the test set to the pharmacophore hypothesis were visualized and the fit values of the best-fitting conformers were determined (Table 2, see Fig. 3 of the supplementary material).

2.3.2. Molecular docking studies and binding conformation

All dock runs were conducted using Discovery Studio 2.5 to investigate the detailed intermolecular interactions between the ligand and the target protein. An automated docking studies were carried out for the test set **3a**–**n** using the reported 3D structure of α_1-AR homology model [23,41]. Interactive docking using CDOCKER protocol was carried out for all the conformers of each compound of the test set **3a**–**n** to the selected active site. Each docked compound was assigned a score according to its binding mode onto the binding site after energy minimization using prepare ligand protocol. The observed binding energies and the corresponding binding mode of interaction taking place between the ligand (test compound) and the receptor (active site of the protein homology model) are listed in Table 2 (Fig. 6).

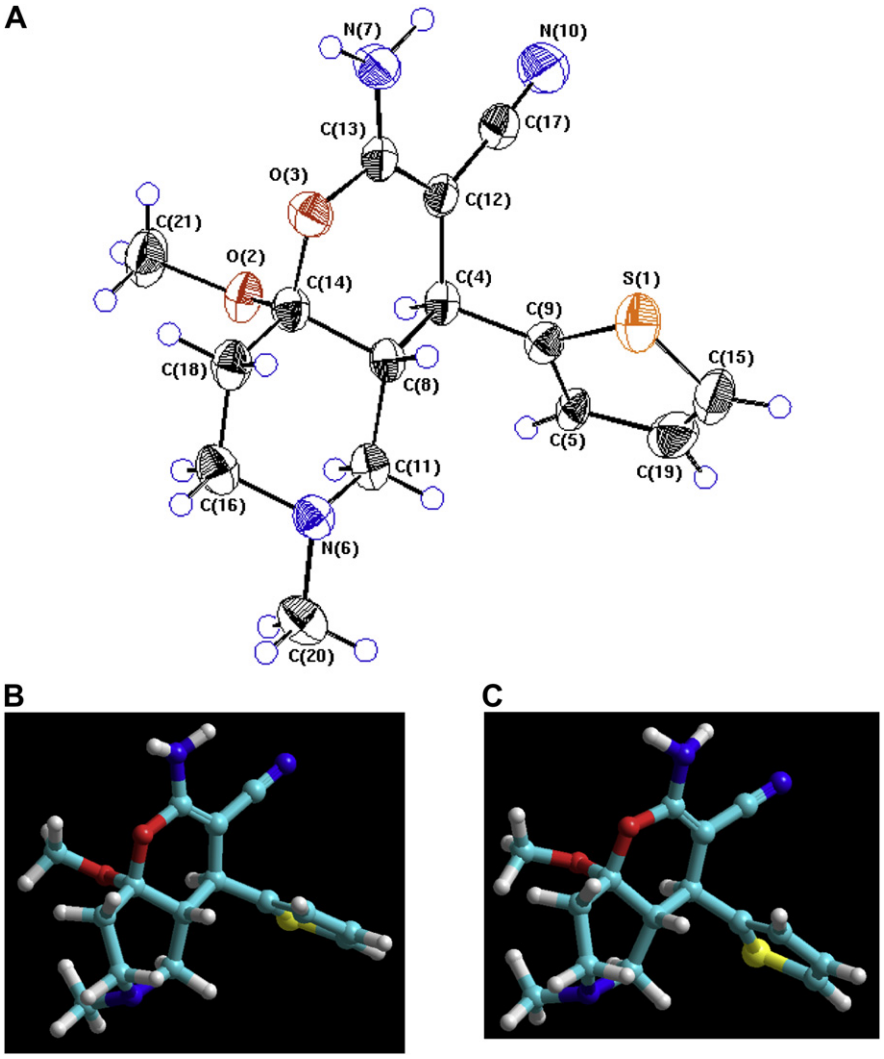

Fig. 5. (A) ORTEP projection of single crystal X-ray diffraction of **3i**; (B), (C) optimized structure of **3i** by semi-empirical AM1 and PM3, respectively.

From the tested compounds mode of interactions with the assigned active site it has been noticed that, compounds **3a**–**c**,**f** possess two hydrogen bonding interactions with both Asp106 and Lys130 amino acids of the active site. However, compounds **3d**,**e**,**j**,**n** possess only one hydrogen bonding interaction with Lys130 amino acid of the active site. Meanwhile, compounds **3i** and **3m** exhibit only one hydrogen bonding interaction with Asp129 amino acid of the active site. On the other hand, compound **3l** observes two hydrogen bonding interactions with both Asp106 and Thr107 amino acids of the active site. Compound **3g** (the most promising vasodilator active agent) has three hydrogen bonding interactions with Asp106 (due to hydrogen atom interaction of amino group attached to 2-position of heterocycle with the carboxylate oxygen of Asp106 amino acid), and two hydrogen bonding interactions with Lys130 (due to oxygen atom interaction of methoxy group attached to phenyl function oriented at the 4-position of the heterocycle and nitrogen atom of the nitrile function with the hydrogen atom of amino function of Lys130). Compound **3h** has no hydrogen bonding interaction with any of the amino acids of the active site (Fig. 6).

Alignment study of docked compound **3g** (the most promising vasodilation active agent) and prazosin (highly selective α_1-AR antagonist) in the binding active pocket of α_1-AR protein homology model revealed that:

i. the *p*-methoxyphenyl residue oriented at the 4-position of **3g** was aligned perfectly with the furanyl moiety of prazosin exhibiting hydrogen bonding interaction with the same amino acid (Lys130) of the active site.
ii. The pyranyl function of **3g** is aligned with the piperazinyl residue of prazosin, where the hydrogen bonding interaction exhibited by the amino group attached to 2-position of heterocycle with the Asp106 of the active site assists greatly for preservation of this oriented alignment.
iii. The distance between the positive ionizable center of compound **3g** which is the heterocyclic nitrogen (*N*-6) and negative edge of Asp106, which is the carboxylate oxygen was more or less similar to that between the nitrogen atom of the prazosin piperazinyl nucleus and the same Asp106 carboxylate oxygen (5.10 and 4.64 Å, respectively) (Fig. 6P).

3. Conclusion

From all the above it could be concluded that, reaction of 1-alkyl-4-piperidones with ylidenemalononitriles in methanol in the presence of sufficient amount of sodium proceeds smoothly affording 6-alkyl-2-amino-4-aryl-4*a*,5,6,7,8,8*a*-hexahydro-8*a*-methoxy-4*H*-pyrano[3,2-*c*]pyridine-3-carbonitriles in good yields (58–73%). The synthesized compounds exhibit promising vasodilation properties

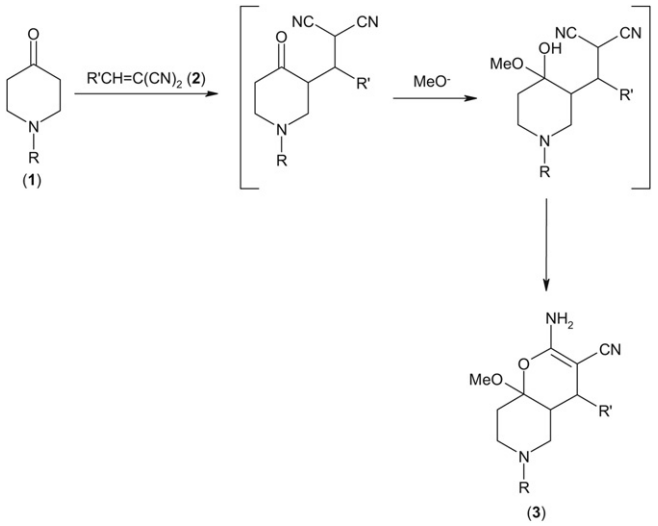

Scheme 2.

especially, **3g** and **3c** which reveal the best vasodilation potency among all the prepared analogues. Molecular modeling studies, including fitting of the synthesized compounds to a 3D-pharmacophore and their docking into optimized homology model as α_1-AR antagonists show high docking score and fit values. The experimental vasodilation activities of compounds **3a**–**n** are consistent with their molecular modeling results. Alignment study of docked compound **3g** (most effective vasodilation active agent) and prazosin (highly selective α_1-AR antagonist lead active agent) in the binding active pocket of α_1-AR protein homology model supports our predicated structure–activity relationships. Where, the *p*-methoxyphenyl residue oriented at the 4-position of **3g** was observed to be aligned perfectly with the furanyl moiety of prazosin exhibiting hydrogen bonding interaction with the same amino acid (Lys130) of the active site, explaining the importance of substitution type attached to the phenyl group oriented at the 4-position of pyrano[3,2-*c*]pyridine-3-carbonitriles in developing the total observed vasorelaxation properties.

4. Experimental

Melting points were recorded on digital Electrothermal 9100 and Stuart SMP3 melting point instruments. IR spectra (KBr) were recorded on a JASCO FT/IR 460-plus spectrophotometer. NMR spectra were recorded on a Varian MERCURY 300 (^{1}H: 300, ^{13}C: 75 MHz) spectrometer. The starting compounds **2a**–**h** [34,42–46] were prepared according to the previously reported procedures.

Table 1
Concentration of compounds necessary to reduce maximal norepinephrine-induced contracture by 50% (IC_{50}) in rat thoracic aortic rings.

Entry	Compound	R	R′	Potency (IC_{50}), mM
1	**3a**	Me	Ph	0.72
2	**3b**	Et	Ph	0.68
3	**3c**	Me	4-ClC_6H_4	0.37
4	**3d**	Et	4-ClC_6H_4	0.40
5	**3e**	Me	4-FC_6H_4	0.52
6	**3f**	Me	4-$H_3CC_6H_4$	0.60
7	**3g**	Me	4-$H_3COC_6H_4$	0.30
8	**3h**	Et	4-$H_3COC_6H_4$	0.68
9	**3i**	Me	2-Thienyl	0.68
10	**3j**	Et	2-Thienyl	0.49
11	**3k**	Me	4-(1-Piperidinyl) phenyl	0.45
12	**3l**	Et	4-(1-Piperidinyl) phenyl	0.48
13	**3m**	Me	4-(4-Morpholinyl) phenyl	0.74
14	**3n**	Et	4-(4-Morpholinyl) phenyl	0.64
15	Prazosin hydrochloride	–	–	0.49

Table 2
Best fit and docking conformer for each compound in the test set (**3a**–**n**) mapped with generated α_1-AR antagonist pharmacophore and active binding pocket of homology model.

Entry	Compound	R	R′	Fit value	Docking value (kcal/mol)
1	**3a**	Me	Ph	2.77	−23
2	**3b**	Et	Ph	3.00	−25
3	**3c**	Me	4-ClC_6H_4	4.10	−32
4	**3d**	Et	4-ClC_6H_4	3.91	−28
5	**3e**	Me	4-FC_6H_4	2.92	−22
6	**3f**	Me	4-$H_3CC_6H_4$	3.00	−26
7	**3g**	Me	4-$H_3COC_6H_4$	4.30	−35
8	**3h**	Et	4-$H_3COC_6H_4$	2.82	−21
9	**3i**	Me	2-Thienyl	2.94	−20
10	**3j**	Et	2-Thienyl	3.00	−28
11	**3k**	Me	4-(1-Piperidinyl) phenyl	3.91	−30
12	**3l**	Et	4-(1-Piperidinyl) phenyl	3.80	−28
13	**3m**	Me	4-(4-Morpholinyl) phenyl	2.80	−18
14	**3n**	Et	4-(4-Morpholinyl) phenyl	2.99	−20
15	Prazosin hydrochloride	–	–	4.21	−33

*4.1. Synthesis of 6-alkyl-2-amino-4-aryl-4a,5,6,7,8,8a-hexahydro-8a-methoxy-4H-pyrano[3,2-c]pyridine-3-carbonitriles **3a**–**n** (general procedure)*

A mixture of equimolar amounts of the appropriate **1a**,**b** and the corresponding **2a**–**h** (10 mmol) in methanol (25 ml) containing sodium (0.46 g, 20 mmol) was stirred at room temperature (20–25 °C) for 24 h. The separated solid was collected, washed with water and crystallized from a suitable solvent affording **3a**–**n**.

*4.1.1. 2-Amino-4a,5,6,7,8,8a-hexahydro-8a-methoxy-6-methyl-4-phenyl-4H-pyrano[3,2-c]pyridine-3-carbonitrile (**3a**)*

Colorless crystals from n-butanol, mp 253–255 °C, yield 67%. IR: ν_{max}/cm^{-1} 3408, 3295 (NH_2), 2174 (C≡N), 1652, 1605 (C=C). ^{1}H NMR (DMSO-d_6): δ 1.65 (dt, 1H, upfield *H*-8, J = 4.5, 13.2, 17.4 Hz), 1.78–1.90 (m, 2H, upfield *H*-5 + *H*-4a), 1.94–2.02 (m, 1H, upfield *H*-7), 2.04 (s, 3H, NCH_3), 2.14–2.16 (m, 1H, downfield *H*-8), 2.24–2.28 (m, 1H, downfield *H*-5), 2.64–2.68 (m, 1H, downfield *H*-7), 3.19–3.23 (m, 1H, *H*-4), 3.28 (s, 3H, OCH_3), 6.35 (s, 2H, NH_2), 7.17–7.35 (m, 5H, arom. H). Anal. Calcd. for $C_{17}H_{21}N_3O_2$ (299.38): C, 68.21; H, 7.07; N, 14.04. Found: C, 68.42; H, 7.21; N, 14.26.

*4.1.2. 2-Amino-6-ethyl-4a,5,6,7,8,8a-hexahydro-8a-methoxy-4-phenyl-4H-pyrano[3,2-c]pyridine-3-carbonitrile (**3b**)*

Colorless crystals from n-butanol, mp 242–244 °C, yield 70%. IR: ν_{max}/cm^{-1} 3404, 3291 (NH_2), 2176 (C≡N), 1649, 1606 (C=C). ^{1}H NMR ($CDCl_3$): δ 0.94 (t, 3H, NCH_2CH_3, J = 7.2 Hz), 1.78 (dt, 1H, upfield *H*-8, J = 4.5, 13.8, 18.0 Hz), 1.93–2.04 (m, 2H, upfield *H*-5 + *H*-4a), 2.06 (heptate, 1H, upfield *H*-7, J = 2.4, 11.4, 13.8 Hz), 2.25–2.41 (m, 3H, downfield *H*-8 + NCH_2CH_3), 2.44–2.47 (m, 1H, downfield *H*-5), 2.83–2.90 (m, 1H, downfield *H*-7), 3.34–3.37 (m, 4H, *H*-4 + OCH_3), 4.39 (s, 2H, NH_2), 7.18–7.35 (m, 5H, arom. H). Anal. Calcd. for $C_{18}H_{23}N_3O_2$ (313.40): C, 68.98; H, 7.40; N, 13.41. Found: C, 69.14; H, 7.51; N, 13.60.

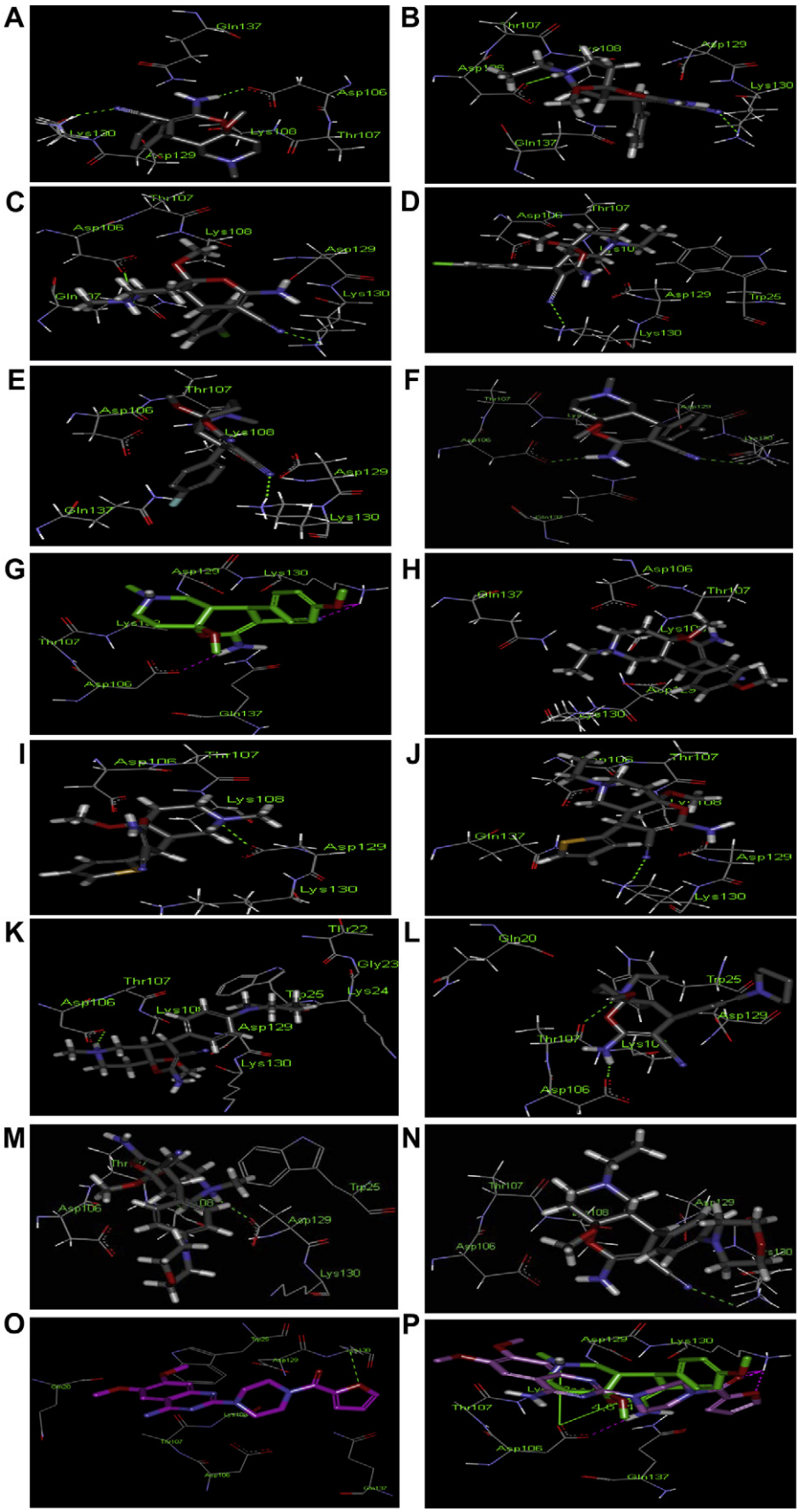

Fig. 6. (A–N) Docking of compounds **3a**–**n**, respectively (O) prazosin into the generated homology model of α_1-AR, (P) alignment of docked compound **3g** (green) and prazosin (magenta) into the active binding site.

*4.1.3. 2-Amino-4-(4-chlorophenyl)-4a,5,6,7,8,8a-hexahydro-8a-methoxy-6-methyl-4H-pyrano[3,2-c]pyridine-3-carbonitrile (**3c**)*

Colorless crystals from n-butanol, mp 251–253 °C, yield 69%. IR: ν_{max}/cm^{-1} 3396, 3292 (NH_2), 2184 (C≡N), 1648, 1607 (C=C). ^{1}H NMR ($CDCl_3$): δ 1.79 (dt, 1H, upfield *H*-8, *J* = 4.5, 13.5, 18.0 Hz), 1.88–1.99 (m, 2H, upfield *H*-5 + *H*-4a), 2.11 (heptate, 1H, upfield *H*-7, *J* = 2.4, 11.4, 13.8 Hz), 2.19 (s, 3H, NCH_3), 2.28 (dt, 1H, downfield *H*-8, *J* = 2.4, 4.8, 13.8 Hz), 2.34–2.37 (m, 1H, downfield *H*-5), 2.72–2.78 (m, 1H, downfield *H*-7), 3.33–3.37 (m, 4H, *H*-4 + OCH_3), 4.43 (s, 2H, NH_2), 7.14 (d, 2H, arom. H, *J* = 8.7 Hz), 7.30 (d, 2H, arom. H, *J* = 8.4 Hz). ^{13}C NMR "on-resonance & APT" (DMSO-d_6): δ 29.7 (*C*-8), 37.9 (*C*-4), 45.0 (*C*-4a), 45.3 (NCH_3), 48.1 (OCH_3), 51.3 (*C*-7), 54.8 (*C*-5), 57.1 (*C*-3), 99.4 (*C*-8a), 120.8 (*C*≡N), 128.2 (*C*-3′), 130.0 (*C*-2′), 131.3 (*C*-4′), 140.9 (*C*-1′), 161.4 (*C*-2). Anal. Calcd. for $C_{17}H_{20}ClN_3O_2$ (333.82): C, 61.17; H, 6.04; N, 12.59. Found: C, 60.93; H, 5.88; N, 12.39.

*4.1.4. 2-Amino-4-(4-chlorophenyl)-6-ethyl-4a,5,6,7,8,8a-hexahydro-8a-methoxy-4H-pyrano[3,2-c]pyridine-3-carbonitrile (**3d**)*

Almost colorless crystals from n-butanol, mp 240–242 °C, yield 72%. IR: ν_{max}/cm^{-1} 3399, 3287 (NH_2), 2182 (C≡N), 1646, 1607 (C=C). ^{1}H NMR (DMSO-d_6): δ 0.83 (t, 3H, NCH_2CH_3, *J* = 7.2 Hz), 1.61 (br t, 1H, upfield *H*-8), 1.76–1.99 (m, 3H, upfield *H*-5 + *H*-4a + upfield *H*-7), 2.21–2.29 (m, 4H, NCH_2CH_3 + downfield *H*-8 + downfield *H*-5), 2.75–2.79 (m, 1H, downfield *H*-7), 3.22–3.31 (m, 4H, *H*-4 + OCH_3), 6.40 (s, 2H, NH_2), 7.23 (dd, 2H, arom. H, *J* = 2.7, 8.4 Hz), 7.37 (dd, 2H, arom. H, *J* = 2.7, 8.4 Hz). ^{13}C NMR "on-resonance" (DMSO-d_6): δ 11.9 (NCH_2CH_3), 29.7 (*C*-8), 38.0 (*C*-4), 45.4 (*C*-4a), 48.20 (OCH_3), 48.29 (NCH_2CH_3), 50.9 (*C*-7), 52.6 (*C*-5), 57.0 (*C*-3), 99.8 (*C*-8a), 121.0 (*C*≡N), 128.3 (*C*-3′), 130.1 (*C*-2′), 131.3 (*C*-4′), 141.0 (*C*-1′), 161.5 (*C*-2). Anal. Calcd. for $C_{18}H_{22}ClN_3O_2$ (347.85): C, 62.15; H, 6.38; N, 12.08. Found: C, 62.06; H, 6.25; N, 11.97.

*4.1.5. 2-Amino-4-(4-fluorophenyl)-4a,5,6,7,8,8a-hexahydro-8a-methoxy-6-methyl-4H-pyrano[3,2-c]pyridine-3-carbonitrile (**3e**)*

Colorless crystals from n-butanol, mp 246–248 °C, yield 69%. IR: ν_{max}/cm^{-1} 3398, 3294 (NH_2), 2183 (C≡N), 1650, 1611 (C=C). ^{1}H NMR ($CDCl_3$): δ 1.79 (dt, 1H, upfield *H*-8, *J* = 4.5, 13.8, 18.0 Hz), 1.88–1.99 (m, 2H, upfield *H*-5 + *H*-4a), 2.11 (heptate, 1H, upfield *H*-7, *J* = 2.4, 11.7, 13.8 Hz), 2.19 (s, 3H, NCH_3), 2.28 (dt, 1H, downfield *H*-8, *J* = 2.4, 5.1, 13.8 Hz), 2.35–2.37 (m, 1H, downfield *H*-5), 2.72–2.78 (m, 1H, downfield *H*-7), 3.34–3.37 (m, 4H, *H*-4 + OCH_3), 4.43 (s, 2H, NH_2), 6.99–7.05 (m, 2H, arom. H), 7.15–7.19 (m, 2H, arom. H). Anal. Calcd. for $C_{17}H_{20}FN_3O_2$ (317.37): C, 64.34; H, 6.35; N, 13.24. Found: C, 64.12; H, 6.29; N, 13.15.

*4.1.6. 2-Amino-4a,5,6,7,8,8a-hexahydro-8a-methoxy-6-methyl-4-(4-methylphenyl)-4H-pyrano[3,2-c]pyridine-3-carbonitrile (**3f**)*

Colorless crystals from n-butanol, mp 238–240 °C, yield 73%. IR: ν_{max}/cm^{-1} 3406, 3293 (NH_2), 2181 (C≡N), 1649, 1604 (C=C). ^{1}H NMR ($CDCl_3$): δ 1.79 (dt, 1H, upfield *H*-8, *J* = 4.5, 13.5, 18.0 Hz), 1.90–2.02 (m, 2H, upfield *H*-5 + *H*-4a), 2.11 (heptate, 1H, upfield *H*-7, *J* = 2.7, 11.4, 13.8 Hz), 2.18 (s, 3H, NCH_3), 2.27 (dt, 1H, downfield *H*-8, *J* = 2.4, 5.1, 13.8 Hz), 2.33 (s, 3H, $ArCH_3$), 2.38–2.42 (m, 1H, downfield *H*-5), 2.71–2.78 (m, 1H, downfield *H*-7), 3.30–3.34 (m, 4H, *H*-4 + OCH_3), 4.39 (s, 2H, NH_2), 7.08 (d, 2H, arom. H, *J* = 8.4 Hz), 7.13 (d, 2H, arom. H, *J* = 8.1 Hz). Anal. Calcd. for $C_{18}H_{23}N_3O_2$ (313.40): C, 68.98; H, 7.40; N, 13.41. Found: C, 68.85; H, 7.29; N, 13.57.

*4.1.7. 2-Amino-4a,5,6,7,8,8a-hexahydro-8a-methoxy-4-(4-methoxyphenyl)-6-methyl-4H-pyrano[3,2-c]pyridine-3-carbonitrile (**3g**)*

Colorless crystals from n-butanol, mp 228–230 °C, yield 67%. IR: ν_{max}/cm^{-1} 3402, 3292 (NH_2), 2186 (C≡N), 1648, 1614 (C=C). ^{1}H NMR ($CDCl_3$): δ 1.78 (dt, 1H, upfield *H*-8, *J* = 4.5, 13.8, 18.0 Hz), 1.88–1.98 (m, 2H, upfield *H*-5 + *H*-4a), 2.10 (heptate, 1H, upfield *H*-7, *J* = 2.4, 11.4, 13.8 Hz), 2.17 (s, 3H, NCH_3), 2.26 (dt, 1H, downfield *H*-8, *J* = 2.4, 5.1, 13.8 Hz), 2.37–2.40 (m, 1H, downfield *H*-5), 2.70–2.76 (m, 1H, downfield *H*-7), 3.28–3.32 (m, 4H, *H*-4 + OCH_3), 3.79 (s, 3H, OCH_3), 4.45 (s, 2H, NH_2), 6.85 (d, 2H, arom. H, *J* = 8.7 Hz), 7.11 (d, 2H, arom. H, *J* = 8.7 Hz). Anal. Calcd. for $C_{18}H_{23}N_3O_3$ (329.40): C, 65.63; H, 7.04; N, 12.76. Found: C, 65.40; H, 6.96; N, 12.68.

*4.1.8. 2-Amino-6-ethyl-4a,5,6,7,8,8a-hexahydro-8a-methoxy-4-(4-methoxyphenyl)-4H-pyrano[3,2-c]pyridine-3-carbonitrile (**3h**)*

Colorless crystals from n-butanol, mp 207–208 °C, yield 70%. IR: ν_{max}/cm^{-1} 3342, 3295 (NH_2), 2186 (C≡N), 1652, 1608 (C=C). ^{1}H NMR (DMSO-d_6): δ 0.83 (t, 3H, NCH_2CH_3, *J* = 7.5 Hz), 1.60 (br t, 1H, upfield *H*-8), 1.73–1.99 (m, 3H, upfield *H*-5 + *H*-4a + upfield *H*-7), 2.19–2.28 (m, 4H, NCH_2CH_3 + downfield *H*-8 + downfield *H*-5), 2.75–2.78 (m, 1H, downfield *H*-7), 3.14–3.24 (m, 1H, *H*-4), 3.27 (s, 3H, OCH_3), 3.74 (s, 3H, OCH_3), 6.29 (s, 2H, NH_2), 6.87 (dd, 2H, arom. H, *J* = 2.1, 8.4 Hz), 7.10 (dd, 2H, arom. H, *J* = 2.1, 8.4 Hz). Anal. Calcd. for $C_{19}H_{25}N_3O_3$ (343.43): C, 66.45; H, 7.34; N, 12.24. Found: C, 66.64; H, 7.54; N, 12.13.

*4.1.9. 2-Amino-4a,5,6,7,8,8a-hexahydro-8a-methoxy-6-methyl-4-(2-thienyl)-4H-pyrano[3,2-c]pyridine-3-carbonitrile (**3i**)*

Colorless crystals from n-butanol, mp 245–247 °C, yield 69%. IR: ν_{max}/cm^{-1} 3420, 3291 (NH_2), 2174 (C≡N), 1651, 1601 (C=C). ^{1}H NMR (DMSO-d_6): δ 1.65 (dt, 1H, upfield *H*-8, *J* = 4.2, 13.2, 17.7 Hz), 1.78–1.89 (m, 2H, upfield *H*-5 + *H*-4a), 1.94–2.02 (m, 1H, upfield *H*-7), 2.09 (s, 3H, NCH_3), 2.23–2.28 (m, 1H, downfield *H*-8), 2.32–2.34 (m, 1H, downfield *H*-5), 2.66–2.70 (m, 1H, downfield *H*-7), 3.27 (s, 3H, OCH_3), 3.56–3.59 (m, 1H, *H*-4), 6.44 (s, 2H, NH_2), 6.92–6.95 (m, 2H, thienyl *H*-3, *H*-4), 7.40–7.42 (m, 1H, thienyl *H*-5). ^{13}C NMR "on-resonance" (DMSO-d_6): δ 29.6 (*C*-8), 34.0 (*C*-4), 45.2 (*C*-4a), 46.4 (NCH_3), 48.3 (OCH_3), 51.3 (*C*-7), 55.1 (*C*-5), 58.1 (*C*-3), 99.4 (*C*-8a), 120.7 (*C*≡N), 124.8 (*C*-5′), 126.1 (*C*-3′), 126.4 (*C*-4′), 146.0 (*C*-2′), 161.0 (*C*-2). Anal. Calcd. for $C_{15}H_{19}N_3O_2S$ (305.40): C, 58.99; H, 6.27; N, 13.76. Found: C, 59.09; H, 6.33; N, 13.85.

*4.1.10. 2-Amino-6-ethyl-4a,5,6,7,8,8a-hexahydro-8a-methoxy-4-(2-thienyl)-4H-pyrano[3,2-c]pyridine-3-carbonitrile (**3j**)*

Almost colorless crystals from n-butanol, mp 228–230 °C, yield 72%. IR: ν_{max}/cm^{-1} 3406, 3292 (NH_2), 2176 (C≡N), 1651, 1600 (C=C). ^{1}H NMR (DMSO-d_6): δ 0.86 (t, 3H, NCH_2CH_3, *J* = 7.2 Hz), 1.62 (dt, 1H, upfield *H*-8, *J* = 4.2, 13.2, 17.4 Hz), 1.75–2.00 (m, 3H, upfield *H*-5 + *H*-4a + upfield *H*-7), 2.24–2.30 (m, 3H, NCH_2CH_3 + downfield *H*-8), 2.40–2.43 (m, 1H, downfield *H*-5), 2.77–2.80 (m, 1H, downfield *H*-7), 3.27 (s, 3H, OCH_3), 3.58 (d, 1H, *H*-4, *J* = 10.8 Hz), 6.43 (s, 2H, NH_2), 6.92–6.95 (m, 2H, thienyl *H*-3, *H*-4), 7.40–7.42 (m, 1H, thienyl *H*-5). Anal. Calcd. for $C_{16}H_{21}N_3O_2S$ (319.43): C, 60.16; H, 6.63; N, 13.15. Found: C, 60.00; H, 6.46; N, 13.35.

*4.1.11. 2-Amino-4a,5,6,7,8,8a-hexahydro-8a-methoxy-6-methyl-4-[4-(1-piperidinyl)phenyl]-4H-pyrano[3,2-c]pyridine-3-carbonitrile (**3k**)*

Yellow crystals from methanol, mp 238–240 °C, yield 65%. IR: ν_{max}/cm^{-1} 3336, 3130 (NH_2), 2189 (C≡N), 1660, 1594 (C=C). ^{1}H NMR ($CDCl_3$): δ 1.52–1.83 (m, 7H, 3 piperidinyl CH_2 + upfield *H*-8), 1.86–1.98 (m, 2H, upfield *H*-5 + *H*-4a), 2.09 (heptate, 1H, upfield *H*-7, *J* = 2.7, 11.4, 13.8 Hz), 2.17 (s, 3H, NCH_3), 2.26 (dt, 1H, downfield *H*-8, *J* = 2.4, 5.1, 13.8 Hz), 2.40–2.43 (m, 1H, downfield *H*-5), 2.71–2.76 (m, 1H, downfield *H*-7), 3.14 (t, 4H, 2 piperidinyl NCH_2, *J* = 5.4 Hz), 3.24–3.27 (m, 1H, *H*-4), 3.32 (s, 3H, OCH_3), 4.39 (s, 2H, NH_2), 6.87 (d, 2H, arom. H, *J* = 8.7 Hz), 7.05 (d, 2H, arom. H, *J* = 8.7 Hz). Anal. Calcd. for $C_{22}H_{30}N_4O_2$ (382.51): C, 69.08; H, 7.91; N, 14.65. Found: C, 69.17; H, 7.98; N, 14.76.

*4.1.12. 2-Amino-6-ethyl-4a,5,6,7,8,8a-hexahydro-8a-methoxy-4-[4-(1-piperidinyl)phenyl]-4H-pyrano[3,2-c]pyridine-3-carbonitrile (**3l**)*

Yellow crystals from n-butanol, mp 231–233 °C, yield 58%. IR: ν_{max}/cm^{-1} 3357, 3127 (NH_2), 2183 (C≡N), 1654, 1594 (C=C). ^1H NMR ($CDCl_3$): δ 1.01 (t, 3H, NCH_2CH_3, $J = 7.2$ Hz), 1.53–1.74 (m, 6H, 3 piperidinyl CH_2) 1.88–2.22 (m, 4H, upfield *H*-8 + *H*-4a + upfield *H*-5 + upfield *H*-7), 2.30 (dt, 1H, downfield *H*-8, $J = 2.4$, 4.8, 14.1 Hz), 2.43 (q, 2H, NCH_2CH_3, $J = 7.2$ Hz), 2.57–2.60 (m, 1H, downfield *H*-5), 2.95–2.98 (m, 1H, downfield *H*-7), 3.14 (t, 4H, 2 piperidinyl NCH_2, $J = 5.7$ Hz), 3.24–3.27 (m, 1H, *H*-4), 3.33 (s, 3H, OCH_3), 4.42 (s, 2H, NH_2), 6.88 (dd, 2H, arom. H, $J = 2.1$, 6.9 Hz), 7.05 (dd, 2H, arom. H, $J = 2.1$, 6.9 Hz). Anal. Calcd. for $C_{23}H_{32}N_4O_2$ (396.54): C, 69.67; H, 8.13; N, 14.13. Found: C, 69.84; H, 8.22; N, 14.34.

*4.1.13. 2-Amino-4a,5,6,7,8,8a-hexahydro-8a-methoxy-6-methyl-4-[4-(4-morpholinyl)phenyl]-4H-pyrano[3,2-c]pyridine-3-carbonitrile (**3m**)*

Pale yellow crystals from methanol, mp 241–243 °C, yield 60%. IR: ν_{max}/cm^{-1} 3340, 3122 (NH_2), 2185 (C≡N), 1659, 1594 (C=C). ^1H NMR ($CDCl_3$): δ 2.12–2.40 (m, 8H, upfield *H*-8 + upfield *H*-5 + *H*-4a + upfield *H*-7 + NCH_3 + downfield *H*-8), 2.67 (br s, 1H, downfield *H*-5), 3.07 (br s, 1H, downfield *H*-7), 3.16 (t, 4H, 2 morpholinyl NCH_2, $J = 4.8$ Hz), 3.27–3.30 (m, 1H, *H*-4), 3.36 (s, 3H, OCH_3), 3.85 (t, 4H, 2 morpholinyl OCH_2, $J = 4.5$ Hz), 4.51 (s, 2H, NH_2), 6.88 (d, 2H, arom. H, $J = 8.4$ Hz), 7.11 (d, 2H, arom. H, $J = 8.7$ Hz). Anal. Calcd. for $C_{21}H_{28}N_4O_3$ (384.48): C, 65.60; H, 7.34; N, 14.57. Found: C, 65.81; H, 7.50; N, 14.38.

*4.1.14. 2-Amino-6-ethyl-4a,5,6,7,8,8a-hexahydro-8a-methoxy-4-[4-(4-morpholinyl)phenyl]-4H-pyrano[3,2-c]pyridine-3-carbonitrile (**3n**)*

Yellow crystals from n-butanol, mp 240–242 °C, yield 68%. IR: ν_{max}/cm^{-1} 3357, 3132 (NH_2), 2183 (C≡N), 1654, 1593 (C=C). ^1H NMR ($CDCl_3$): δ 1.02 (t, 3H, NCH_2CH_3, $J = 7.2$ Hz), 1.95–2.59 (m, 8H, upfield *H*-8 + upfield *H*-5 + *H*-4a + upfield *H*-7 + NCH_2CH_3 + downfield *H*-8 + downfield *H*-5), 2.96–2.99 (m, 1H, downfield *H*-7), 3.15 (t, 4H, 2 morpholinyl NCH_2, $J = 4.5$ Hz), 3.23–3.29 (m, 1H, *H*-4), 3.34 (s, 3H, OCH_3), 3.85 (t, 4H, 2 morpholinyl OCH_2, $J = 4.8$ Hz), 4.44 (s, 2H, NH_2), 6.86 (d, 2H, arom. H, $J = 8.7$ Hz), 7.10 (d, 2H, arom. H, $J = 8.1$ Hz). Anal. Calcd. for $C_{22}H_{30}N_4O_3$ (398.51): C, 66.31; H, 7.59; N, 14.06. Found: C, 66.13; H, 7.39; N, 13.90.

*4.2. Single crystal X-ray crystallographic data of **3c**, **3d** and **3i***

Full crystallographic details, excluding structure factors have been deposited at Cambridge Crystallographic Data Centre (CCDC) as supplementary publication numbers CCDC 813935, 813936 and 813934 for compounds **3c**, **3d** and **3i**, respectively. The crystallographic data were collected at $T = 298$ K on a Kappa CCD Enraf Nonius FR 590 diffractometer using a graphite monochromator with Mo-K_α radiation ($\lambda = 0.71073$ Å). The crystal structures were determined by SIR92 [47] and refined by maXus [48] (Bruker Nonius, Delft and MacScience, Japan).

*4.2.1. Compound **3c***

For X-ray crystallographic studies, compound **3c** was recrystallized as prismatic colorless crystals from n-butanol. Chemical formula $C_{17}H_{20}ClN_3O_2$, $M_r = 333.819$, monoclinic, crystallizes in space group $P2_{1/c}$, Cell lengths "$a = 12.3953(5)$, $b = 7.8570(3)$, $c = 19.2974(12)$ Å", Cell angles "$\alpha = 90.00$, $\beta = 116.21(18)$, $\gamma = 90.00°$", $V = 1686.07(14)$ Å^3, $Z = 4$, $D_c = 1.315$ mg/m^3, θ values 2.910–21.967°, absorption coefficient μ (Mo-K_α) = 0.24 mm^{-1}, $F(000) = 704$. The unique reflections measured 6778 of which 1312 reflections with threshold expression $I > 3\sigma(I)$ were used in the structural analysis. Convergence for 208 variable parameters by least-squares refinement on F^2 with $w = 1/[\sigma^2(F_o^2) + 0.10000F_o^2]$. The final agreement factors were $R = 0.042$ and $wR = 0.076$ with a goodness-of-fit of 1.778.

*4.2.2. Compound **3d***

For X-ray crystallographic studies, compound **3d** was recrystallized as cubic colorless crystals from ethanol. Chemical formula $C_{18}H_{22}ClN_3O_2$, $M_r = 347.846$, monoclinic, crystallizes in space group $P2_{1/c}$, Cell lengths "$a = 12.5220(5)$, $b = 8.0160(3)$, $c = 19.3366(9)$ Å", Cell angles "$\alpha = 90.00$, $\beta = 12.(18) \times 10^{1^\circ}$, $\gamma = 90.00°$", $V = 1724.58$ (12) Å^3, $Z = 4$, $D_c = 1.340$ mg/m^3, θ values 2.910–26.373°, absorption coefficient μ (Mo-K_α) = 0.24 mm^{-1}, $F(000) = 736$. The unique reflections measured 3809 of which 2107 reflections with threshold expression $I > 3\sigma(I)$ were used in the structural analysis. Convergence for 217 variable parameters by least-squares refinement on F^2 with $w = 1/[\sigma^2(F_o^2) + 0.10000F_o^2]$. The final agreement factors were $R = 0.041$ and $wR = 0.073$ with a goodness-of-fit of 1.365.

*4.2.3. Compound **3i***

For X-ray crystallographic studies, compound **3i** was recrystallized as prismatic colorless crystals from ethanol. Chemical formula $C_{15}H_{19}N_3O_2S$, $M_r = 305.400$, monoclinic, crystallizes in space group $P2_{1/c}$, Cell lengths "$a = 12.8283(5)$, $b = 8.0250(2)$, $c = 18.9020(7)$ Å", Cell angles "$\alpha = 90.00$, $\beta = 13.(18) \times 10^{1^\circ}$, $\gamma = 90.00°$", $V = 1524.23$ (9) Å^3, $Z = 4$, $D_c = 1.331$ mg/m^3, θ values 2.910–30.034°, absorption coefficient μ (Mo-K_α) = 0.22 mm^{-1}, $F(000) = 648$. The unique reflections measured 4569 of which 2493 reflections with threshold expression $I > 3\sigma(I)$ were used in the structural analysis. Convergence for 190 variable parameters by least-squares refinement on F^2 with $w = 1/[\sigma^2(F_o^2) + 0.10000F_o^2]$. The final agreement factors were $R = 0.072$ and $wR = 0.155$ with a goodness-of-fit of 2.165.

4.3. Vasodilation properties screening

The vasodilation activity screening procedures were carried out according to the standard reported techniques [23–25,39,40] by testing the effects of the synthesized pyrano[3,2-*c*]pyridine-3-carbonitrile derivatives (**3a**–**n**) on isolated thoracic aortic rings of male Wister rats (250–350 g). After light ether anaesthesia, the rats were sacrificed by cervical dislocation. The aortae were immediately excised, freed of extraneous tissues and prepared for isometric tension recording. Aorta was cut into (3–5 mm width) rings and each ring was placed in a vertical chamber "10 ml jacketed automatic multi-chamber organ bath system (Model no. ML870B6/C, Panlab, Spain)" filled with Krebs solution composed of (in mM): NaCl, 118.0; KCl, 4.7; $NaHCO_3$, 25.0; $CaCl_2$, 1.8; NaH_2PO_4, 1.2; $MgSO_4$, 1.2; glucose, 11.0 and oxygenated with carbogen gas (95% O_2/5% CO_2) at 37 ± 0.5 °C. Each aortic ring was mounted between two stainless steel hooks passed through its lumen. The lower hook was fixed between two plates, while the upper one was attached to a force displacement transducer (Model no. MLT0201, Panlab, Spain) connected to an amplifier (PowerLab, AD Instruments Pty. Ltd.) which is connected to a computer. The Chart for windows (v 3.4) software was used to record and elaborate data.

Preparations were stabilized under 2 g resting tension during 2 h and then the contracture response to norepinephrine hydrochloride (10^{-6} M) was measured before and after exposure to increasing concentrations of the tested synthesized compounds. The tested compounds were dissolved in dimethylsulfoxide (DMSO) as stock solution (10 ml of 0.01 M). Control experiments were performed in the presence of DMSO alone, at the same concentrations as those used with the tested derivatives, which demonstrated that the solvent did not affect the contractile response of isolated aorta. Means of three successive runs were used to extract the

experimental data. The observed vasodilation activity screening data are reported (Table 1, see also Figs. 1, 2 of the supplementary material) and the potency (IC_{50}, concentration necessary for 50% reduction of maximal norepinephrine hydrochloride induced contracture) was determined by the best fit line technique.

Acknowledgment

This study was supported financially by the Science and Technology Development Fund (STDF), Egypt, Grant No. 1357. Thanks are also to Pharmacology Department, NRC, Cairo, Egypt, for allowing performance of pharmacological activity screening.

Appendix A. Supplementary material

Supplementary data associated with this article can be found, in the online version, at doi:10.1016/j.ejmech.2011.03.023.

References

[1] K.A. Jackman, O.L. Woodman, C.G. Sobey, Curr. Med. Chem. 14 (2007) 2824–2838.
[2] I. Husedzinovic, N. Bradic, T. Goranovic, Signa Vitae 1 (2006) 9–12.
[3] J.W.E. Rush, S.G. Denniss, D.A. Graham, Can. J. Appl. Physiol. 304 (2005) 442–474.
[4] A. Koenig, C. Roegler, K. Lange, A. Daiber, E. Glusa, J. Lehmann, Bioorg. Med. Chem. Lett. 17 (2007) 5881–5885.
[5] X. Dong, Y. Liu, J. Yan, C. Jiang, J. Chen, T. Liu, Y. Hu, Bioorg. Med. Chem. 16 (2008) 8151–8160.
[6] G.S. Stokes, J. Clin. Hypertens. (Greenwich) 6 (2004) 192–197.
[7] A.V. Chobanian, G.L. Bakris, H.R. Black, W.C. Cushman, L.A. Green, J.L. Izzo Jr., D.W. Jones, B.J. Materson, S. Oparil, J.T. Wright Jr., E.J. Roccella, JAMA 289 (2003) 2560–2572.
[8] A.E. Kümmerle, J.M. Raimundo, C.M. Leal, G.S. da Silva, T.L. Balliano, M.A. Pereira, C.A. de Simone, R.T. Sudo, G. Zapata-Sudo, C.A.M. Fraga, E.J. Barreiro, Eur. J. Med. Chem. 44 (2009) 4004–4009.
[9] T. Yamanaka, M. Yasumoto, T. Nakajima, O. Yaoka, Chem. Abstr. 118 (1993) 169097 Jpn. Kokai Tokkyo Koho JP 04,282,353 (92,282,353) (Cl. C07C239/20), 7 Oct. 1992.
[10] M. Baumgarth, R. Gericke, I. Lues, J. De Peyer, R. Bergmann, Chem. Abstr. 111 (1989) 97213 Eur. Pat. Appl. EP 308,792 (Cl. C07D491/04), 29 Mar. 1989.
[11] J.M. Evans, G. Stemp, F. Cassidy, Chem. Abstr. 106 (1987) 213921 Eur. Pat. Appl. EP 205,292 (Cl. C07D491/04), 17 Dec. 1986.
[12] A.R. Katritzky, A.S. Girgis, S. Slavov, S.R. Tala, I. Stoyanova-Slavova, Eur. J. Med. Chem. 45 (2010) 5183–5199.
[13] A.S. Girgis, F.F. Barsoum, A. Samir, Eur. J. Med. Chem. 44 (2009) 2447–2451.
[14] F.F. Barsoum, A.S. Girgis, Eur. J. Med. Chem. 44 (2009) 2172–2177.
[15] A.S. Girgis, F.F. Barsoum, Eur. J. Med. Chem. 44 (2009) 1972–1977.
[16] A.S. Girgis, Eur. J. Med. Chem. 44 (2009) 1257–1264.
[17] A.S. Girgis, Eur. J. Med. Chem. 44 (2009) 91–100.
[18] A.S. Girgis, Eur. J. Med. Chem. 43 (2008) 2116–2121.
[19] A.S. Girgis, N. Mishriky, M. Ellithey, H.M. Hosni, H. Farag, Bioorg. Med. Chem. 15 (2007) 2403–2413.
[20] A.S. Girgis, M. Ellithey, Bioorg. Med. Chem. 14 (2006) 8527–8532.
[21] A.S. Girgis, H.M. Hosni, F.F. Barsoum, Bioorg. Med. Chem. 14 (2006) 4466–4476.
[22] F.F. Barsoum, H.M. Hosni, A.S. Girgis, Bioorg. Med. Chem. 14 (2006) 3929–3937.
[23] A.S. Girgis, N.S.M. Ismail, H. Farag, W.I. El-Eraky, D.O. Saleh, S.R. Tala, A.R. Katritzky, Eur. J. Med. Chem. 45 (2010) 4229–4238.
[24] A.S. Girgis, A. Kalmouch, M. Ellithey, Bioorg. Med. Chem. 14 (2006) 8488–8494.
[25] A.S. Girgis, N. Mishriky, A.M. Farag, W.I. El-Eraky, H. Farag, Eur. J. Med. Chem. 43 (2008) 1818–1827.
[26] M.A. Mahran, Alexandria J. Pharm. Sci. 15 (2001) 149–151 Chem. Abstr. 137 (2002) 149771.
[27] H.I. El-Subbagh, S.M. Abu-Zaid, M.A. Mahran, F.A. Badria, A.M. Al-Obaid, J. Med. Chem. 43 (2000) 2915–2921.
[28] M.A. Al-Omar, K.M. Youssef, M.A. El-Sherbeny, S.A.A. Awadalla, H.I. El-Subbagh, Arch. Pharm. (Weinheim, Germany) 338 (2005) 175–180.
[29] R.R. Kumar, S. Perumal, P. Senthilkumar, P. Yogeeswari, D. Sriram, Bioorg. Med. Chem. Lett. 17 (2007) 6459–6462.
[30] A.S. Girgis, H.M. Hosni, A. Kalmouch, J. Chem. Res. (2005) 38–40.
[31] A.S. Girgis, I.S. Ahmed-Farag, Z. Naturforsch. 58b (2003) 698–703.
[32] N. Mishriky, Y.A. Ibrahim, A.S. Girgis, N.G. Fawzy, Pharmazie 55 (2000) 269–272.
[33] N. Mishriky, F.M. Asaad, Y.A. Ibrahim, A.S. Girgis, J. Chem. Res. (S) (1997) 316–317.
[34] N. Mishriky, F.M. Asaad, Y.A. Ibrahim, A.S. Girgis, Recl. Trav. Chim. Pays-Bas. 113 (1994) 35–39.
[35] M.J.S. Dewar, E.G. Zoebisch, E.F. Healey, J.J.P. Stewart, J. Am. Chem. Soc. 107 (1985) 3902–3909.
[36] J.J.P. Stewart, Comput. Chem. 10 (1989) 209–220.
[37] J.J.P. Stewart, Comput. Chem. 10 (1989) 221–264.
[38] P. Machado, P.T. Campos, G.R. Lima, F.A. Rosa, A.F.C. Flores, H.G. Bonacorso, N. Zanatta, M.A.P. Martins, J. Mol. Struct. 917 (2009) 176–182.
[39] J.M. Raimundo, R.T. Sudo, L.B. Pontes, F. Antunes, M.M. Trachez, G. Zapata-Sudo, Eur. J. Pharmacol. 530 (2006) 117–123.
[40] A.G. Silva, G. Zapata-Sudo, A.E. Kummerle, C.A.M. Fraga, E.J. Barreiro, R.T. Sudo, Bioorg. Med. Chem. 13 (2005) 3431–3437.
[41] I.J.A. MacDougall, R. Griffith, J. Mol. Graph. Model. 25 (2006) 146–157.
[42] B.B. Corson, R.W. Stoughton, J. Am. Chem. Soc. 50 (1928) 2825–2837.
[43] H.G. Sturz, C.R. Noller, J. Am. Chem. Soc. 71 (1949) 2949.
[44] M.A. Weinberger, R.M. Heggie, H.L. Holmes, Can. J. Chem. 43 (1965) 2585–2593.
[45] L. Horner, K. Klüpfel, Ann. 591 (1955) 69–98.
[46] J.S.A. Brunskill, A. De, G.M.F. Vas, Synth. Commun. 8 (1978) 1–7.
[47] A. Altomare, G. Cascarano, C. Giacovazzo, A. Guagliardi, M.C. Burla, G. Polidori, M. Camalli, J. Appl. Cryst. 27 (1994) 435–436.
[48] S. Mackay, C.J. Gilmore, C. Edwards, N. Stewart, K. Shankland, maXus Computer Program for the Solution and Refinement of Crystal Structures. Bruker Nonius, The Netherlands, MacScience, Japan, 1999, The University of Glasgow.